Available online at www.sciencedirect.com
SCIENCE DIRECT®
Remote Sensing of Environment 98 (2005) 388 – 402
Remote Sensing of Environment
www.elsevier.com/locate/rse

Detecting and measuring new snow accumulation on ice sheets by satellite remote sensing

Robert Bindschadler [a,1], Hyeungu Choi [b,*], Christopher Shuman [c], Thorsten Markus [d]

[a] Hydrospheric and Biospheric Sciences Laboratory, NASA Goddard Space Flight Center, Greenbelt, MD 20771, United States
[b] SAIC, Beltsville, MD 20705-2675, United States
[c] Cryospheric Sciences Branch, Hydrospheric and Biospheric Sciences Laboratory, NASA Goddard Space Flight Center, Greenbelt, MD 20771, United States
[d] Instrumentation Sciences Branch, Hydrospheric and Biospheric Sciences Laboratory, NASA Goddard Space Flight Center, Greenbelt, MD 20771, United States

Received 31 March 2005; received in revised form 27 July 2005; accepted 28 July 2005

Abstract

A new technique is described that detects when and where new snow falls on ice sheets and then determines the thickness of new accumulation. Measurements of vertically polarized passive emission at 85 GHz are filtered with the Hilbert–Huang Transform to identify periods where the surface snow has changed significantly. These are shown to be commonly the result of new snow by comparison with both field observations and in situ instrumentation. Temperature, atmospheric emission and clouds all affect the passive microwave signal but each is examined and shown not to prevent the identification of new snow events. The magnitude of the brightness temperature change is not strongly correlated with snowfall amount. To quantify the amount of new snow, the spatial extent and timing of new snowfalls are examined with ICESat/GLAS laser altimetry data. Crossover differences between altimetric profiles taken before, during, and after the snowfall event provide a measure of the thickness of new snow. Specific cases are presented where 11 and 13 cm of new snow were detected over large regions.

Keywords: Snowfall; Ice sheets; Microwave emission; SSMI; ICESat; Snow event

1. Introduction

Snow accumulates on ice sheets to replenish the mass lost by melting and calving. It is a primary component of the mass balance and, as such, figures heavily into whether an ice sheet changes in volume, affecting sea level, and how it makes these adjustments through altered flow and geometry. It is against the record of past accumulation that present patterns and amounts of accumulation are judged to represent significant changes in either climate or weather.

The majority of the Antarctic Ice Sheet is a high elevation polar desert where a single snowfall may deposit only a thin dusting of new snow. Average net annual accumulation can be as low as 3 cm water equivalent (about 10 cm of snow at a density of 0.3 g/cm^3) (Giovinetto & Zwally, 2000). Indeed, field reports exist from places where no accumulation was received for more than a year and the surface may actually lower through ablation aided by wind scour and densification. Larger snowfalls and annual accumulations are more characteristic of the perimeters of the Antarctic ice sheet and much of its smaller, Greenland sibling.

Despite its importance, the details of snow accumulation on the scale of an ice sheet are poorly known. Great effort has been expended by many people over many years in measuring accumulation amounts in ice cores, snow pits, trenches and with surface stakes or automated acoustic sounders. The universal limitation of these methods is that the data are restricted to a small area and time period. Ice flow introduces an additional complexity because older accumulated snow extracted at depth via an ice core originates upstream from the sample site (except for stable ice domes) and it is well known that surface topographic variations have a strong influence on accumulation (Black & Budd, 1964; Gow & Rowland, 1965; and Whillans, 1975). The pervasiveness of both the spatial and temporal variability

* Corresponding author. Tel.: +1 301 614 5707; fax: +1 301 614 5666.
E-mail addresses: Robert.A.Bindschadler@nasa.gov (R. Bindschadler), choi@ice.gsfc.nasa.gov (H. Choi).
[1] Tel.: +1 301 614 5664.

0034-4257/$ - see front matter © 2005 Elsevier Inc. All rights reserved.
doi:10.1016/j.rse.2005.07.014

Fig. 1. Location of study areas in Antarctica: Siple Dome (star); McMurdo Station (triangle); and Dronning Maud Land (square).

of ice sheet accumulation has been most recently demonstrated by high-frequency radars towed along the surface that map continuous near-surface layers (Arcone et al., in press; Richardson & Holmlund, 1999). Compilations of accumulation measurements have had to rely on significant interpolations and extrapolations to produce maps of annual accumulation across the vastness of the ice sheets (Bales et al., 2001; Giovinetto & Zwally, 2000; Vaughan et al., 1999). Modeling results can suffer from the same temporal and spatial sampling issues because models frequently use field observations to 'tune' model parameters (Bromwich et al., 2001).

Here we present a new method to identify the extent and timing of new snow on an ice sheet using passive microwave data followed by a quantitative estimate of the amount of new snow across the area by multiple laser altimetric measurements. The technique is based on the observation that the vertically polarized emission at 85 GHz changes when the very top of the snowpack has been altered. By appropriate filtering of these data, we derive a time series that is dominated by the surface signal and is insensitive to unwanted effects caused by passing meteorological systems. These two sensors work independent of solar illumination, so we expect the method to work in all seasons. We make use of direct field observations of weather conditions, including snowfall, and automatic instruments at numerous sites (Fig. 1) to demonstrate the general success of our approach. Once the location and timing of new snow is identified, we use ICESat altimetry data to quantify any change in surface elevation.

2. Identification of snowfall events

2.1. Concept

Our detection approach is designed to identify new snow once it has fallen, not while it is falling. Identification of falling snow particles against a background of snow is expected to be extremely difficult, if not intractable, with current satellite sensors and the temporal frequency of satellite observations might miss entire snowfall events. Our methodology to identify new snow once it had fallen and laid on the surface employs strengths of current sensors, but is not without its own difficulties, as we discuss below.

Our approach employs passive microwave data to detect a difference between old snow that has laid on the surface for some time and new, fresh snow. Snow crystals form in the atmosphere in a variety of shapes, depending on the temperature and pressure conditions during condensation of water vapor onto nucleating surfaces (Nakaya, 1954). Lacy dendrites are most familiar, but other forms, such as platelets, columns or needles, are more commonly formed in the cold, dry conditions above ice sheets. After deposition, they immediately begin to change, diminishing their angularity to form larger, more rounded snow grains. This metamorphic process is ubiquitous and driven by many factors, including temperature, vertical temperature gradients, overlying pressure, humidity, and even wind.

2.2. Passive microwave emission

Emission of microwave energy from an object depends on the temperature of the object and its ability to emit, which is determined by its internal scattering properties. Emissions from deeper within an object are attenuated more because of the additional intervening material.

Satellite measurements of the passive microwave emission of the Earth began in 1973. The usual observation frequencies are at or near 6, 19, 23, 37 GHz, with 85 GHz added in 1987, corresponding to spectral windows in atmospheric absorption. Our approach uses the data collected at 85 GHz (3.5 mm wavelength) by the SSM/I sensor for two primary reasons: first, the radiation emitted from the ice sheet at this frequency originates at and very near the surface; and second, there is a long heritage of measurements at this frequency that makes it likely such measurements will be continued into the foreseeable future.

Estimates and measurements of penetration depth of microwaves into polar snow have been made (e.g., Rott et al., 1993). Penetration depth shows a clear decrease with increasing frequency, but the measurements do not extend to 85 GHz. Tedesco (pers. comm.) used a dense medium radiative theory model to extend the measurements to this higher frequency with the result that for snow parameters that reproduced the lower frequency penetration depths reported in the literature, 85 GHz energy would have a penetration depth of 2 centimeters.

Emissions at frequencies higher than 85 GHz, i.e. at or near 183 GHz, have been used to sound the atmosphere for ice or water particles (Skofronick-Jackson et al., 2004). However, precipitating snow is not distinguishable from cirrus clouds over an ice sheet. Lower frequencies (i.e. 37 GHz and longer wavelengths) are insensitive to clouds, but also less sensitive to the surface properties as they integrate over more of the underlying snowpack.

Satellite passive microwave data are usually collected at both vertical and horizontal polarization. Over the ice sheets, we observed very few differences between the temporal

variations of brightness temperature records for the horizontal and vertical polarizations at 85 GHz with the horizontal polarization being a nearly constant 17 K lower than the vertical polarization. Fig. 2 presents an example of 85 GHz brightness temperature from Siple Dome (81.67° S, 149.07° W, 600 m.a.s.l.) a site in West Antarctica, situated between two ice streams and adjacent to the Ross Ice Shelf (Fig. 1). Horizontally polarized waves leaving the snowpack are usually attenuated more due to reflections at nearly horizontal stratigraphic horizons both internally and at the surface (Shuman et al., 1993). We use the vertically polarized channel at 85 GHz, termed "85V" from here on, to avoid any complexity caused by near-surface snowpack stratigraphy, which can change over time.

2.3. Methodology

Metamorphism of the surface snow toward rounder snow grains will cause a gradual decrease in emission. New snow deposited on the surface is expected to cause a sudden increase in surface emissivity similar to vertically polarized brightness temperature increases when hoar is buried under new snow (Shuman & Alley, 1993). Our method is based on detecting when and where these increases occur.

It is worth discussing some of the exceptions to this general tendency for surface snow to become more rounded. Hoarfrost is a very delicate and finely structured crystal type that forms on the surface of the snowpack (or any surface) by direct condensation of water vapor. Wind can rapidly break the delicate structures, but in persistent calm conditions, hoarfrost has been observed over very large areas of the surface (Shuman & Alley, 1993) and layers several centimeters thick can form and be buried and preserved by new accumulation (Shuman et al., 1997). We consider hoarfrost as another form of new accumulation because it is derived from atmospheric water vapor not part of the ice sheet prior to deposition.

Wind is another process that influences both snow on the ground and falling through the air. Strong winds can transport snow horizontally while rounding grains through collisions and drive grains closer together forming denser wind crusts. By rounding grains, this process should also decrease microwave emission.

2.4. Effect of physical temperature

The 85V brightness temperatures are the product of the emissivity, itself an index of the scattering within the medium, and the temperature of the emitting material. Gradient ratios, where a normalized difference is calculated between two different microwave channels, have proven useful in sea ice, snow and ice sheet studies as a means to minimize temperature effects (e.g., Abdalati & Steffen, 1997; Cavalieri et al., 1984; Goita et al., 2003). In our case, however, gradient ratios were ineffective in removing the temperature dependence and had the undesirable effect of removing all indications of new snow.

The short-term temporal variations of 85V brightness temperatures are much stronger than the variations of the longer wavelength channels of either 19 or 37 GHz because of the differences in penetration depths. Often the longer wavelength brightness temperatures exhibit a phase delay due to the time it takes a temperature change to reach the deeper layers important to the emission at the lower frequencies. Fig. 2 illustrates these differences by comparing the records of 85V and the vertically polarized channel of 37 GHz at the Siple Dome location for approximately 2 months at the end of 2001. Some cold troughs in the 85-GHz record appear a day later in

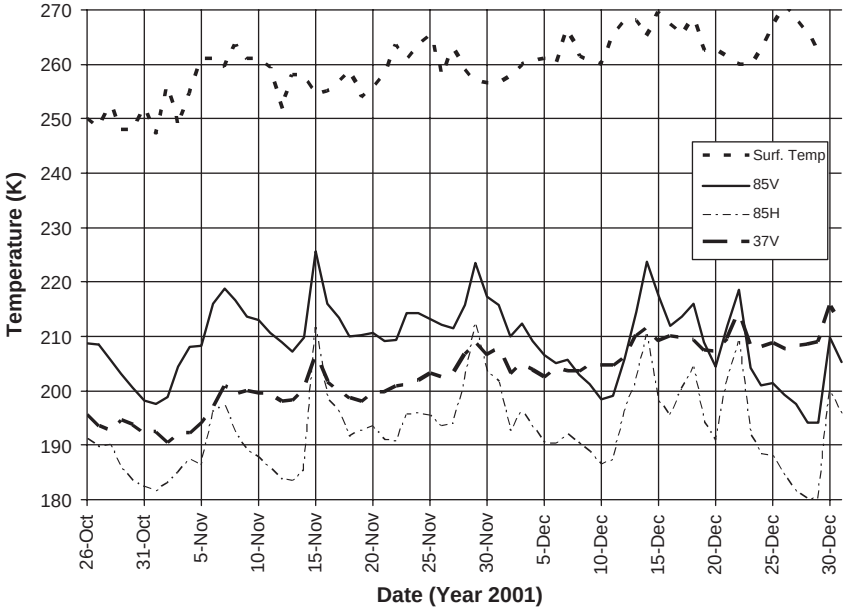

Fig. 2. Daily-averaged passive microwave brightness temperature at 85 GHz vertical and horizontal polarization and at 37 GHz vertical polarization for the pixel including Siple Dome, West Antarctica (in Kelvin, left scale) and mean daily near-surface air temperatures recorded at Siple Dome. Time period shown is October 26, 2001 to December 31, 2001.

the 37-GHz record, the magnitude of the variations are smaller at 37 GHz than at 85 GHz, and 37 GHz exhibit an overall increase in brightness temperature over the 3-month record that is absent in the 85 GHz. Shuman et al. (1997) have shown that the 37V record can be a long-term temperature proxy whereas the 85 GHz is clearly not. All these differences prevent a gradient ratio involving 85 GHz from effectively reducing the physical temperature effect on brightness temperature.

We explored other means to routinely acquire the surface temperature without success. Satellite-based thermal data are collected, but actual surface measurements are available only when cloud is absent yet new snow falls from clouds. Atmospheric models to derive a surface temperature beneath clouds exist, but do not agree well with field data (J. Key, pers. comm.). New snow falls from clouds, so the surface temperatures are needed most when they are least accurate. To be most useful, surface temperatures would be simultaneous with the passive microwave observations.

Diurnal temperature variation is damped and smoothed because we use daily-averaged brightness temperatures gridded to a 12.5-km polar stereographic grid (distributed by the National Snow and Ice Data, Boulder, CO). At high latitudes, there are typically around four measurements per day for a grid cell (less towards the equator, more towards the poles). We examined swath data and found similar correlations to those shown here. We chose to use gridded data because it was easier to complete the continental scale analyses presented later.

2.5. Effect of clouds and atmospheric water vapor

With increasing frequency, the contribution of the atmosphere to the brightness temperature increases with increasing frequency. Clouds and water vapor are the primary sources of this additional scattering and emission. For this reason, algorithms employing 85 GHz data to study sea ice need to account for atmospheric effects usually through the combination with data from other frequencies (e.g. Kaleschke et al., 2001; Markus & Burns, 1995; Markus & Cavalieri, 2000; Svendsen et al., 1987). However, in our case, the magnitude of the atmospheric contribution at 85 GHz was expected to be small relative to the surface emission given the height of the ice sheet surface (which eliminates the lower layers of the atmosphere) and the very cold temperatures over ice sheets (which limits the amount of water vapor contained within the atmosphere) (D. Staelin, pers. comm.). Thus, there was reason to expect 85 GHz data alone could be used for our purpose of new snow detection.

The meteorological observations at Siple Dome allow us to examine the sensitivity to typical cloud conditions over the interior ice sheet. Fig. 3 repeats the record of 85V at Siple Dome camp and compares it with periods when overcast, broken, or scattered cloud covers were observed and when new snow was observed. These field observations were made at least every 6 h (hourly when aircraft were operating nearby). The instances of largest increases in 85V occur when new snow was observed (this point is discussed later). Of more value in examining the effect of clouds alone on the 85V signal are instances when cloud conditions were alternatively overcast, broken or scattered but new snow did *not* occur. Specific cases of this occur on November 20 and 23 and December 3, 6 and 17–18, 2001. In each of these cases, the effect of clouds amounts to less than 4 K and often much less. Many of these modest increases in 85V brightness temperature are removed by our filtering method and do not create a false indication of new snow, however, some false indications of new snow remain.

The contribution of the more dispersed atmospheric emission to the 85V at-satellite signal is examined using radiosonde data collected at McMurdo Station and an atmospheric radiative transfer model (Kummerow, 1993). Measured temperatures (air and dewpoint) were input to the model along with a constant surface emissivity of 0.8. In Fig. 4, the model's prediction of the at-satellite 85V signal is compared with the surface temperature, the satellite-measured

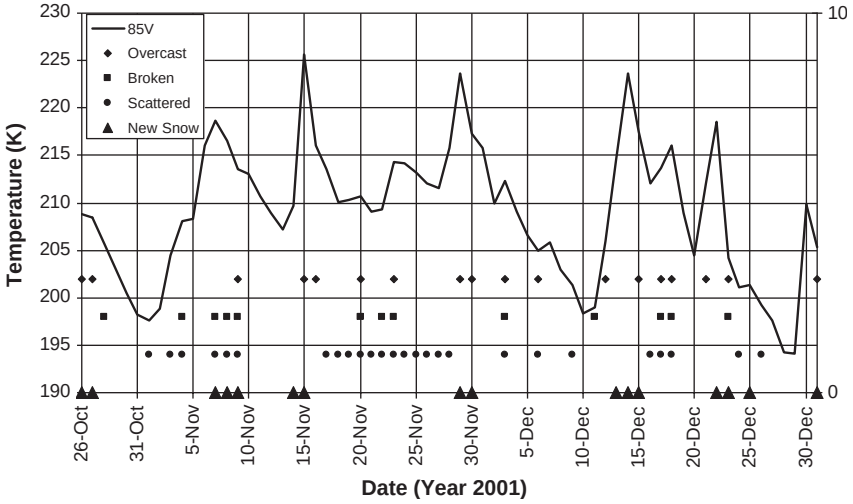

Fig. 3. Daily-averaged 85 GHz vertical polarization brightness temperatures, and accumulated observations of cloud and new snow at Siple Dome, West Antarctica from October 26, 2001 to December 31, 2001. Only the heaviest types of cloud cover: overcast; broken and scattered are included. Triangles indicate days when new snow was observed.

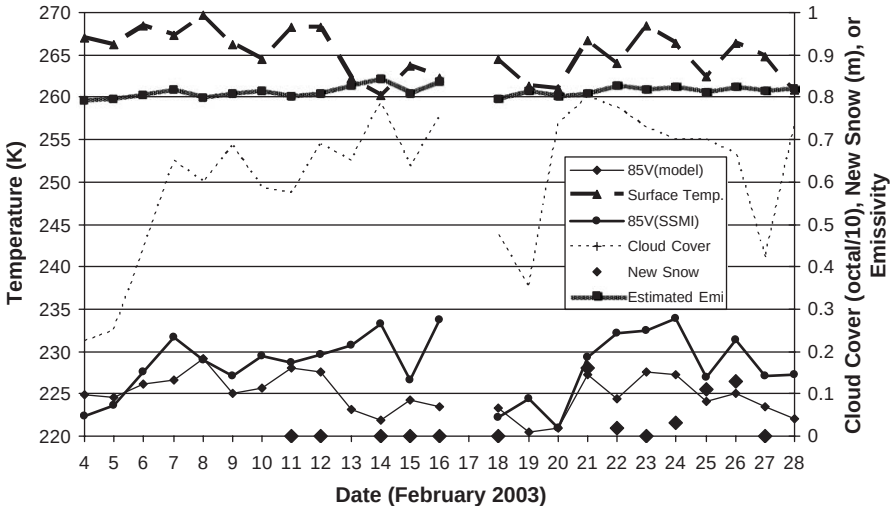

Fig. 4. Measured, observed and calculated conditions at or in the vicinity of McMurdo Station in the month of February 2003. Measurements include the 85 GHz vertically polarized brightness temperatures and the surface temperature (lowest radiosonde measurement); observations include average daily cloud cover (in octals) and new snow occurrence (by amount); and calculations include the at-satellite brightness temperature from a radiative transfer model driven by radiosonde measurements and the effective surface emissivity that would be needed to match the at-satellite brightness temperatures from the atmospheric model with the satellite measurement.

brightness temperature, and observations of both cloud cover and new snow precipitation for most of February 2003. Modeled at-satellite brightness temperatures are strongly correlated with surface temperatures. This is due to the fact that the lowest layers of the atmosphere are warmest and contain the majority of emitting water vapor, even when significant cloud cover is present. During the periods of least cloud cover, the model predictions of the at-satellite brightness temperatures agree well with the measurements.

For more extensive cloud cover, the measured 85V are generally higher than the model predictions with the largest differences, up to 20 K, during periods when new snow was observed. This result supports our contention that the changes in the surface emissivity can be detected despite the separate influence of the atmosphere. Fig. 4 includes the results of a recursive calculation of the apparent surface emissivity required by the model to match the atmospheric model results with the 85V data. The periods of elevated surface emissivity (above 0.82) correspond with periods of new snow. In general, a 0.01 increase in emissivity caused a 0.2-K increase in the atmospheric contribution to brightness temperature.

An important discovery of this analysis was that the net contribution of the atmosphere to 85V is relatively constant. For the 24 days of February, the atmospheric contribution was 13 ± 1 K. Similar results (not shown) were obtained for analyses of the months of November 2003 and August 2003. For the winter month of August 2003, the average surface temperatures were roughly 20 K colder yet the atmosphere contributed a relatively constant 10 ± 0.6 K with a day-to-day variation usually less than 5 K. We conclude from this analysis that temperature variations have a significantly greater impact on the day-to-day variations of 85V than do variations in atmospheric water content (with or without clouds).

3. Time series filtering

Snowfall is a meteorological event driven by atmospheric dynamics on the time scale of days to weeks. Various filtering schemes were explored to reach a product derived from the daily-averaged 85V data that correlated well with available observations of new snow accumulation. These included high-pass filtering, to remove the seasonal temperature variation, low-pass filtering, to remove aliasing caused by nonperiodic sampling at some of the lower latitudes that are less frequently sampled, and band-pass filtering, to remove variations of the 85V data series on time scales other than the 3–7 days typical of the movements and effects of mesoscale storms in the atmosphere.

In the end, we used the Hilbert–Huang Transform (HHT) (Huang, 1998). The HHT has the advantage over other frequency filters, such as bandpass filters or wavelets, that it allows the frequency components to change at every point along the data series. This proved to be a valuable characteristic in our case. Our experience with bandpass filters was that the dominant temporal variation resulting from any choice of bandpass parameters always corresponded to the longest wavelength of the bandpass. This is expected for any data series with decreasing power at shorter wavelengths.

The HHT method produces a set of Intrinsic Mode Functions (IMF) of decreasing numerical significance, each with a zero mean. The first mode contains the highest frequency oscillations while in our cases the highest modes contained the annual and longer cycles. Our choice of what modes to combine for a useful indicator of new snow was empirical. Guided by 3 years of observations of snowfall at McMurdo Station, Antarctica, discussed below, the combination of IMFs 2, 3 and 4 produced the best correlation with observed new snow accumulation events. This choice eliminated the highest frequency variations of 85V as well as the

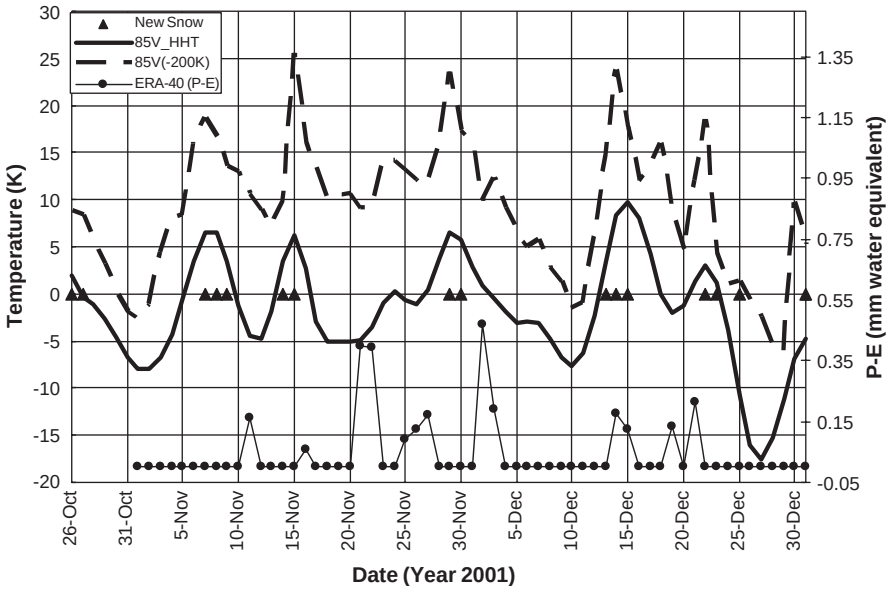

Fig. 5. Daily-averaged 85 GHz vertical polarization brightness temperatures (offset by 200 K to fit scale), filtered 85V_HHT (see text), ERA-40 net precipitation ($P-E$) amounts and observed new snow at Siple Dome, West Antarctica from October 26, 2001 to December 31, 2001. (ERA-40 values provided by D. Bromwich, pers. comm.).

annual signal while capturing the few-day time scale of storms in the daily 85V data set.

The 85V brightness temperature time series at Siple Dome during the 2001 austral summer used in Figs. 1 and 2 is shown again in Fig. 5 along with the IMF234 HHT filtered version of this data series. It smoothes the highest frequency oscillations of the original 85V record while preserving the major peaks and troughs. It is these peaks in the 85V_HHT record that the next section demonstrates to identify new snow events. The HHT record sometimes rises before the new snow is observed because we ignore the highest frequency IMF, making the temporal variations of our HHT product more gradual.

4. Field areas

The field data we used to test our method of new snow detection are of two types: direct observation recorded in weather logs and remote observations by acoustic sounders operating autonomously in the field. In expansive, homogeneous areas, local observations can expect to be representative of the larger areas typically sampled from space, however, in meteorologically complex areas direct observations can sometimes fail to give representative values. Examples of both are illustrated in our analysis.

4.1. Siple Dome

Cloud cover observations from this site have been introduced earlier. In addition to the cloud observations, air temperature, wind speed and direction, fog, and falling or blowing snow, were recorded by station personnel frequently during the last 72 days of 2001. The frequency of weather observations varied with planned aircraft operations in the area from a minimum of every 6 h (omitting the 1200Z observation when camp residents usually slept) to hourly observations for up to 16 h when aircraft were expected to operate in the camp vicinity. These weather records were obtained from the Antarctic Meteorological Research Center (AMRC) at the University of Wisconsin.

Fig. 5 includes the times of seven new snow events directly observed at Siple Dome during this 72-day period. Each of these events corresponds to an interval when 85V_HHT is positive. This correlation is striking and lends strong support to the viability of our method of detecting new snow with 85V data collected from space. The second and third events (beginning on November 7 and 14, respectively) are limited to blowing snow, not falling snow, but we feel it is proper to categorize the horizontal delivery of snow as new snow for the purpose of validating our method of detecting changes to the snowpack surface.

Figs. 6 and 7 represent two additional successful examples of new snow detection at Siple Dome for the 1998 and 2004 austral summers. Only one period of positive 85V_HHT, that around January 23, 2004, does not coincide with new snow. We note that the field records became less regular during this period, but cannot be sure that this new snow was missed. The decline of 85V_HHT values at the end of the 1998 is an artifact of the HHT filtering software reaching the end of the time series (Fig. 6).

An independent estimate of precipitation is available from the 40-year European Re-Analysis (ERA-40) product distributed by the European Centre for Medium-Range Weather Forecasts (ECMWF) (http://www.ecmwf.int/research/era/). In Fig. 5, we include the ERA-40 precipitation minus evaporation ($P-E$) values for the grid cell closest to Siple Dome. The agreement with the field observations is not good, supporting our earlier statement that models do not offer a reliable means of identifying accumulation events. In general, the ERA-40 precipitation events correlate more closely with temperature

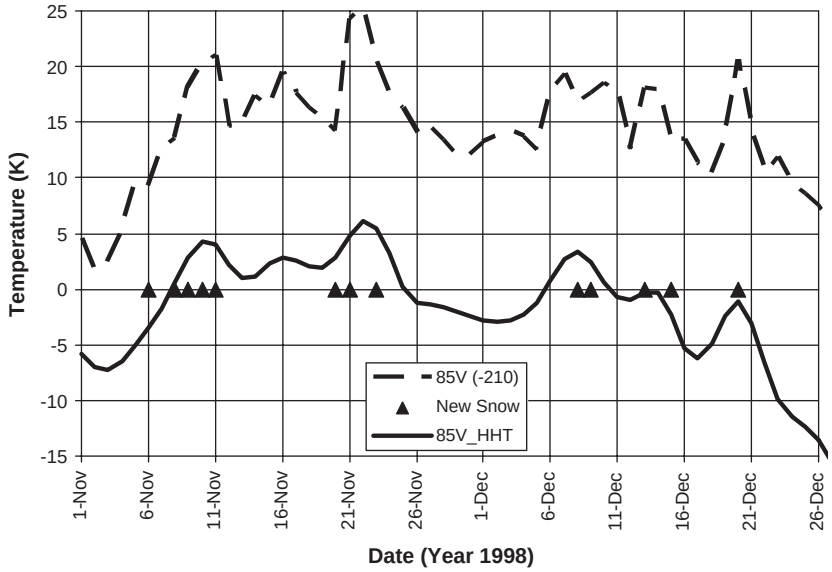

Fig. 6. Daily-averaged 85 GHz vertical polarization brightness temperatures (offset by 210 K to fit scale), filtered 85V_HHT (see text) and observed new snow at Siple Dome, West Antarctica from November 11, 1998 to December 31, 1998.

(see Fig. 2) than with 85V or 85V_HHT. This reinforces our view that while the 85V_HHT time series is affected by temperature, it is not dominated by it and that 85V_HHT record is an effective means to identify new snow events. More instances of the influence on temperature condition are illustrated and discussed later.

4.2. McMurdo Station

This largest Antarctic base is operated year round and is located on Ross Island at 77.92° S, 166.6° E, immediately adjacent to a thin ice shelf (see Fig. 1). McMurdo Station occupies a protected embayment of the island and the topographic variation in the immediate vicinity is large, from the 3794-m summit of Mt. Erebus just 40 km from the station to the local floating ice shelf at the station's edge. We employed five full years (1999–2003) of observations (primarily every 6 h for the observables used here) obtained from the University of Wisconsin AMRC. The amount of new snow was also recorded with "trace" amounts corresponding to less than 0.1 mm (water equivalent). Weather conditions across the island and on the ice shelf can vary enormously on a short spatial scale, undermining the representativeness of weather observations at the station (or at any single point on the island) for our purposes. In addition, we found numerous discrepancies between the daily logs of new snow and the monthly summaries. We chose to rely on the daily records. Despite these shortcomings, we regarded the large number of observa-

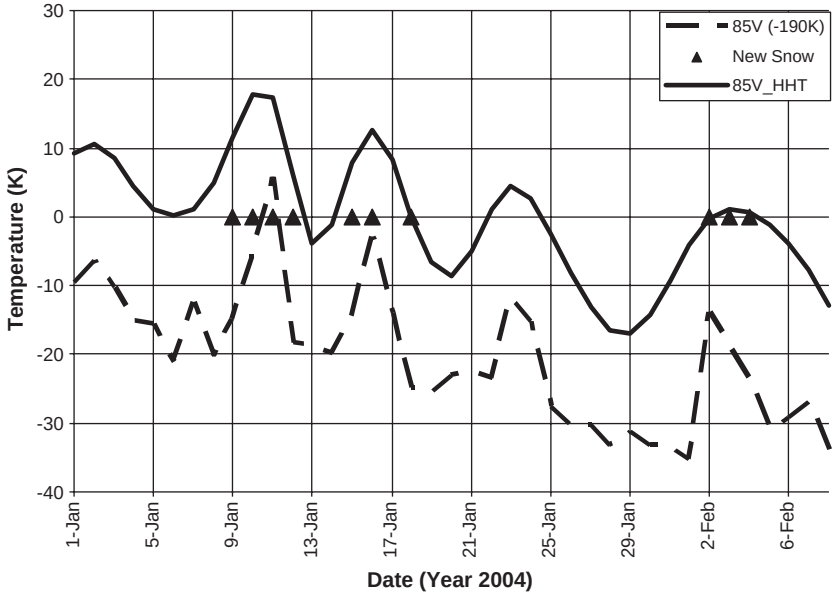

Fig. 7. Daily-averaged 85 GHz vertical polarization brightness temperatures (offset by 190 K to fit scale), filtered 85V_HHT (see text) and observed new snow at Siple Dome, West Antarctica from January 1, 2004 to February 8, 2004.

tions by trained meteorological professionals using standard techniques as a useful data set to test our method.

We formed the 85V time series for the 12.5 × 12.5-km grid cell containing McMurdo Station, decomposed this series with the HHT, formed the 85V_HHT by combining IMFs 2, 3 and 4, and identified the periods of positive 85V_HHT. We then formed a 2 × 2 matrix consisting of cases whether 85V_HHT was either positive or negative versus whether new snow (including trace amounts) occurred during those periods or not. Successful correlation corresponded to periods of positive 85V_HHT that had new snow and periods of negative 85V_HHT that had no snow. Unsuccessful correlation occurred when new snow was observed with negative 85V_HHT or no snow with positive 85V_HHT.

Results for each year were similar. Better correlations were obtained for snow occurrence when trace amounts of snow were not counted as new snow. In 2001, 42 intervals of positive 85V_HHT index occurred with new snow measured in McMurdo during 29 of them: a success rate of 69%. In that same year, no snow was recorded during 47 of the 72 intervals when the 85V_HHT index was negative: a 65% success rate. The success rate over the 5-year interval was 59%.

An alternative indicator that was also examined was to consider a rising HHT signal as an indicator of new snow and a falling HHT an indicator of no snow. This proved extremely successful for the records in 2003: 76% success in predicting new snow (including trace amounts) and 80% success in predicting periods of no snow. However, it performed much worse in other years (sometimes less than 50% success) and overall its performance was below the "positive HHT means snow, negative HHT means no snow" test for the 5-year period.

It is important to reiterate the considerable heterogeneity of the McMurdo area and the spatial mismatch between the 12.5 × 12.5-km size of the 85V grid cell and the very local spatial sample represented by the McMurdo weather observations. It also is worth noting that the positive and negative intervals were defined by local maxima and minima, rather than zero crossings. Therefore, a few instances occurred where two distinct positive intervals were adjacent to each other separated by a local, but positive, minimum value.

It is not possible to be sure that even for the apparent "false positives", i.e., cases where new snow was expected and not observed, that new snow did not occur somewhere within the large 85V pixel. On the other hand, we recognize that our method is conservative and errs on the side of capturing too many episodes of new snow rather than missing any. This bias is deliberate and justified by the expectation that for false positive cases the altimeter-derived measurement of snowfall amount (discussed later) would independently indicate a negligible amount of new snow.

4.3. Comparison with acoustic depth gauges

The second type of field data used to validate our detection method was collected by acoustic sounders operating at various locations in Greenland and Antarctica. This type of sensor measures the local change in height to sub-centimeter precision. The measurement is inherently very local. As an extreme example, at one Greenland site, two identical sensors separated by only 2 m showed instances where one recorded an increase in surface height while the other recorded no change or even a decrease. Thus, although the acoustic sounders do measure changes in the local surface elevation, comparisons with our method that reflect changes over a 12.5 × 12.5-km area are not expected to be perfect.

Reijmer and van den Broeke (2003) reported measurements in Dronning Maud Land, Antarctica where they operated acoustic sounders at a number of sites both at low-elevation, near coastal sites and at higher elevations farther inland (see Fig. 1). Their analysis identified two types of events: low magnitude but more frequent events that were not always observed over the entire instrumented region and larger events that generally were observed by all instruments. They noted that the cumulative magnitude of the more frequent, smaller events was a significant fraction of the total accumulation of an area so they cannot be ignored in terms of accounting for the total accumulation at a site.

In Fig. 8, 6 months of filtered 85V_HHT data are compared with two sounder records, both mounted on the same instrument mast at Saddle station (66.0006° N, 44.5014° W, 2559 m.a.s.l.) in central Greenland (Steffen, pers. comm.). Similar to observations of Reijmer and van den Broeke (2003), the sounder records both indicate a series of accumulation events with magnitudes of over 10 cm and more frequent, smaller events that sometimes only appear on one record (e.g., Day 30). There are times when an accumulation event is followed by a wind erosion event that removes all recent accumulation (e.g., Day 48 or Day 94). Some of the large accumulation events are followed by a gradual sinking of the surface (e.g., Day 17 or Day 158) that is likely due to snow densification.

The periods of positive 85V_HHT do a good job of capturing both the large and the small accumulation events in the acoustic sounder records. Even for cases where only one sounder registers an increase in surface elevation, the 85V_HHT detects a change. There are some instances of "false positives", i.e., a positive 85V_HHT but no surface elevation increase in either sensor (e.g., Day 104). These cases can usually be explained by a relatively large change in temperature (also included in Fig. 8). Such changes in temperature are expected to change the 85V emission even without new snow. As in the McMurdo data set, however, false positives are less common than actual instances of new snow.

The second example, Fig. 9, is taken from a 4-month segment of data collected in Dronning Maud Land (Reijmer, pers. comm.). Their site #6 (74.4814° S, 11.5183° W) is located on the ice shelf and against the rise to the East Antarctic plateau (Reijmer & van den Broeke, 2003) (see Fig. 1). The acoustic sounder records three major snowfalls with the third composed of three distinct sub-events. The 85V_HHT captures all of these events and sub-events, however the middle sub-event (on April 7) is smoothed from the original 85V data. The large increase in 85V_HHT on February 3 matches the large

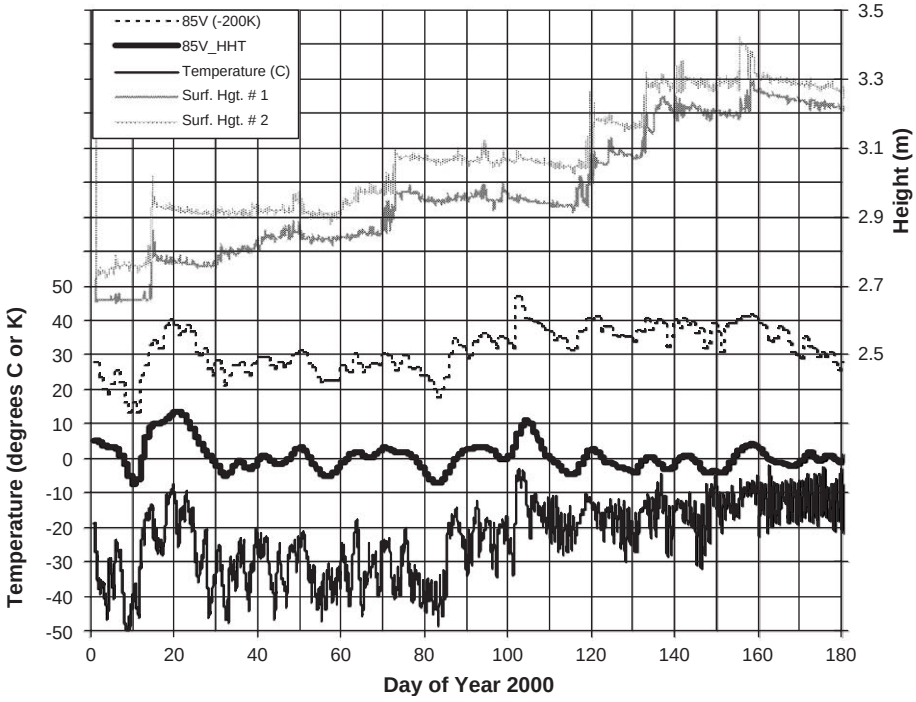

Fig. 8. Surface heights (from acoustic sounders), near-surface air temperatures (in degrees Celsius), 85V brightness temperatures (offset by 200 K to fit scale), filtered 85V_HHT brightness temperatures (in K) at Saddle station in Greenland for the first 180 days of 2000. (Field data provided by K. Steffen, pers. comm.).

20-cm snowfall and gradually decreases while remaining positive for 25 days during which the snow surface elevation subsided without further accumulation. A few minor peaks superimposed on this gradual decline are seen to correlate with short periods of warmer temperatures during the more than 50-day period following this event.

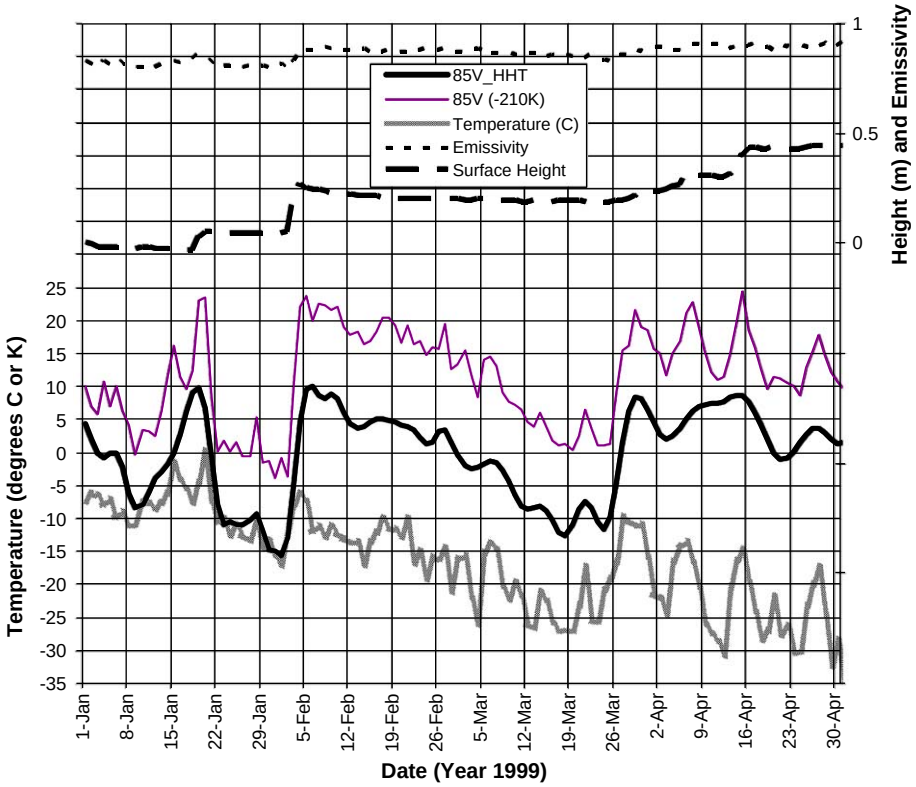

Fig. 9. Surface heights (from acoustic sounder), near-surface air temperatures (in degrees Celsius), 85V brightness temperatures (offset by 210 K to fit scale), filtered 85V_HHT brightness temperatures (in K) and calculated emissivities at site #6 in Dronning Maud Land, Antarctica from January 1, 1999 to April 30, 1999. (Field data provided by C. Reijmer, pers. comm.).

Although the periods of positive 85V_HHT correlate well with occurrence of new snow, the magnitude of 85V_HHT peaks are not strongly correlated with the amount of new snow measured by the sounders. At some other sites with generally lower accumulation, there was a hint that the larger snowfalls were tied to the larger positive swings in 85V_HHT. It is reasonable to expect some threshold of accumulation exists beyond which the covered older snow layers are effectively masked. This threshold might likely be on the order of a few times the roughly 2-cm penetration depth in snow at 85 GHz. When viewed over the broader set of sounder data, however, this correlation does not prove to be a reliable means to estimate new snow depth.

5. Spatial distribution of identified new snow events

Our method is easily applied to every cell of the 12.5-km polar stereographic projection grid. The continuous time series of 85V_HHT, processed for the entire ice sheet of Antarctica and Greenland, can be used to produce animations of new snow events over either ice sheet for any time period for which the 85V data are available. These animations enable the study of the source and evolution of new snow events and illustrate their spatial coherence. Fig. 10 shows a sequence of frames of one such event.

A majority of events sweep in from the coast. Some dissipate at an ice divide. Others originate in the interior of the ice sheet and spread out over millions of square kilometers before dissipating. Overall, the spatial and temporal characters of these events are consistent with mesoscale meteorological processes.

Without showing the entire set of frames for Antarctica and Greenland, one summary parameter that can be extracted and displayed in map view is the number of events at every grid cell for an entire year. Fig. 11 shows that the predicted number of events do vary across Antarctica. As expected, coastal areas experience more precipitation episodes, while the higher elevation interior receives fewer new snow events. Because our method is designed to make errors of commission, i.e., predict new snow when there was not any, rather than errors of omission, i.e., fail to predict new snow when there was some, the frequency of events in Fig. 11 is probably too high rather than too low.

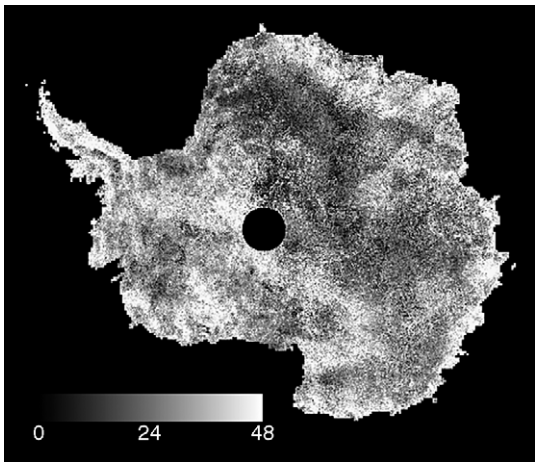

Fig. 11. Number of positive 85V_HHT periods for Antarctica in 2003.

6. Snowfall magnitude from ICESat

To quantify the accumulation amount for an identified snowfall event, we turn to measurements from the very precise Geodynamics Laser Altimeter System (GLAS) on-board the Ice, Cloud and land Elevation Satellite (ICESat). The single-shot precision of this revolutionary space instrument is less than 10 cm (Zwally et al., 2002). As noted earlier, these data are not yet sufficiently accurate to both identify the location and to measure the magnitude of most snowfalls on ice sheets. Therefore, we employ our prediction of the areal extent and timing of individual snow events derived from the 85V_HHT time series to parse the GLAS

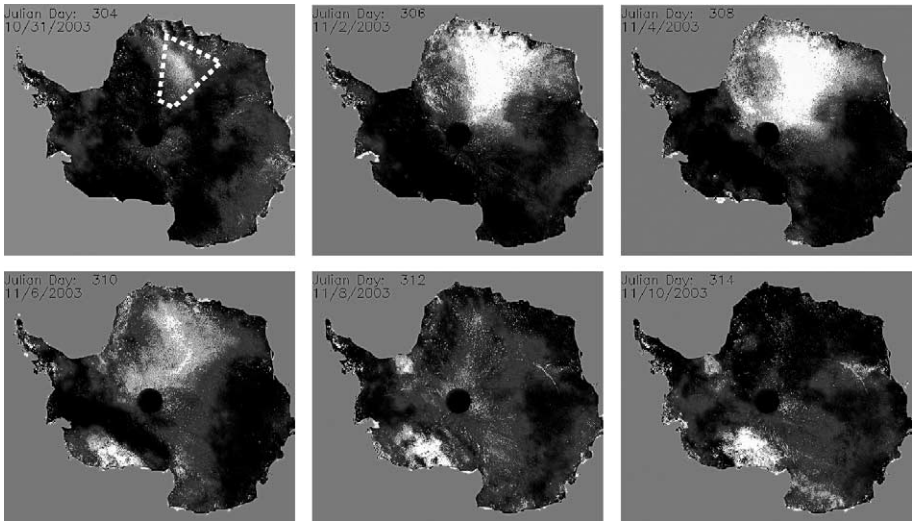

Fig. 10. 85V_HHT event in East Antarctica during 2003. Image shown every other day. Pixel brightness corresponds to value of HHT with higher values (brighter pixels) indicating higher likelihood of new snow. White box indicates area of crossover analysis discussed in text.

data (Release 18) and produce a statistical measure of the increase in surface elevation over the larger new snow region rather than at a single grid cell.

We illustrate this approach for the very extensive new snow event centered on November 2, 2003, in Dronning Maud Land, Antarctica (cf., Fig. 10) when ICESat/GLAS was operating in a

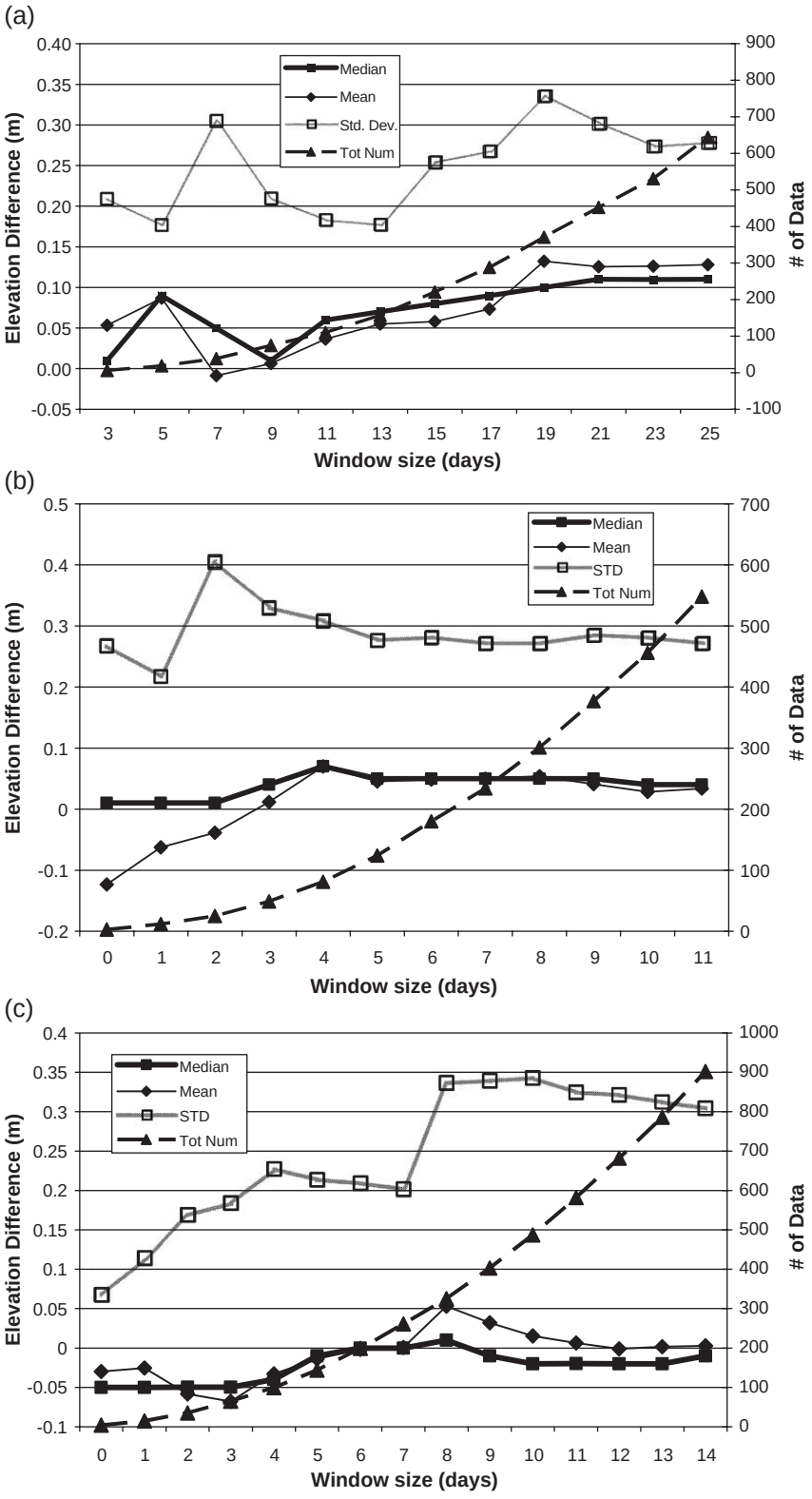

Fig. 12. Statistics of ICESat/GLAS crossover differences for time windows: (a) centered on November 2, 2003 when early pass is before November 2 and later pass is after November 2; (b) before November 2, 2003 when late pass is on this date and early pass is successively earlier than this date: and (c) after November 2, 2003 when early pass is on this date and late pass is successively later than this date.

91-day repeat cycle mode. The box in Fig. 10 indicates the area over which the analysis is performed. The method employs elevation differences at intersections of two altimeter passes. These "crossover differences", or "crossovers" for short, are calculated as the later pass's elevation, linearly interpolated between actual altimeter measurements to the precise location of the crossover point, minus the similarly interpolated elevation for the earlier pass (Zwally & Brenner, 2001). Linear interpolation is required because the laser footprints are 70 m in diameter spaced at intervals of 220 m.

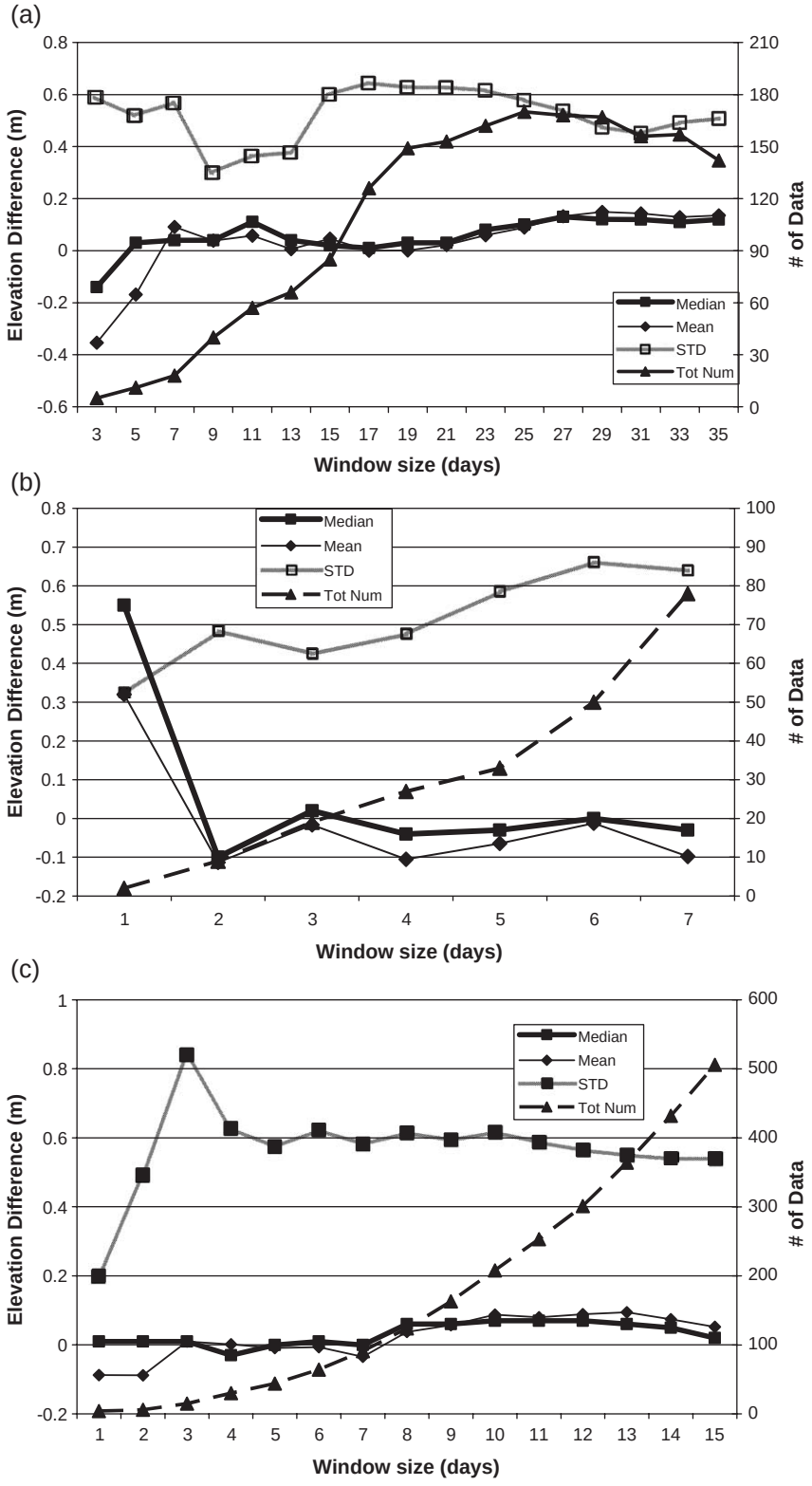

Fig. 13. Statistics of ICESat/GLAS crossover differences for time windows (a) centered, (b) before and (c) after March 1, 2003.

We model the snow event as an instantaneous increase in elevation centered on the date of maximum positive 85V_HHT and form the crossover differences from pass pairs where the earlier pass occurs before the date of the new snow event and the later pass occurs after this date. Both passes must occur within a specified larger time window during which no other significant 85V_HHT activity occurs.

The true change is likely distributed in time and may be spatially variable because our elevation change model is idealized. A series of time windows, each of increasing size and centered on the event date, are considered. This procedure gradually increases the number of crossover elevation differences as well as their temporal separation. Fig. 12(a) shows how the mean, median, standard deviation and number of the crossover elevation differences change as the size of the time window is changed. In this example, both the mean and median crossover differences approach values of between 10 and 15 cm and appear to stabilize for a window size of 21 days (i.e., 10 days on either side of the event date) or more. In all cases, the few crossover differences greater than ±2 m were omitted prior to calculating the statistics. The standard deviation often falls between 20 and 30 cm, but the shape of the distribution is strongly Gaussian, especially for the larger window sizes, suggesting our mean and median values are meaningful.

There are many instrumental sources of error that are compressed into the stated single shot precision of less than 10 cm. These include orbit determination, timing and other time-dependent instrumental biases and surface slope. Under optimum conditions, a precision better than ±3 cm has been demonstrated (Shuman et al., submitted for publication). Atmospheric corrections are continually being improved with better cloud masks to identify those elevations affected by thin clouds that allow a laser altimeter pulse to pass through but delay or "spread" the returning signal causing an artificially low apparent surface elevation. Overall, our standard deviations are in the range of 20 to 30 cm.

As a further check on the effectiveness of our method, we used the same technique to examine the distribution of crossover differences for time windows required to include either both passes before, or both passes after the event time. In either case, one edge of the window was fixed at the snow event date and the window enlarged either to earlier or later times. In the case of the pre-event period (Fig. 12(b)), the mean and median crossover differences converged on a very stable value between 4 and 5 cm. The standard deviations stabilized at about 28 cm, similar to the previous case. In the post-event period, shown in Fig. 12(c), the behavior showed an initial elevation drop measured both in the mean and median, growing to a value near zero for the larger window sizes and, as before, a standard deviation close to 30 cm. We speculate that the initial decrease of elevation in these post-event windows represents the compaction of the new snow layer (cf. Fig. 9) or surface scour, however, we have no supporting data that either explanation is correct.

We applied this same method to a second new snow event seen in our 85V_HHT animation. The event was centered on March 1, 2003, during an 8-day repeat orbit cycle of ICESat. In this case, the box for sampling crossover differences extended from 78° to 84° S and from 20° E to 20° W. Fig. 13 shows that the means and medians for time windows centered on March 1 stabilized near 13 cm while the standard deviations were closer to 50 cm. The pre-event windows produced slightly negative means and medians with standard deviations near 60 cm. The number of crossover differences never exceeded 80 because the proximity of an earlier event limited the size of the largest pre-event window to 7 days. The post-event windows were larger and showed the early negative, then stable behavior as seen in the first example.

We also analyzed a third case that we speculate is a "false positive" example (not shown). Despite adjustments to the selection of the event date, we could not extract a clear accumulation signal for a range of event-centering dates and very large time windows. As we have shown, positive periods of 85V_HHT can be due to other effects such as a wind storm that transports new snow horizontally (seen at Siple Dome), a change in surface temperature (illustrated with the Dronning Maud Land data, Fig. 9), or an actual new snow event that was followed by an erosion event (seen in the acoustic sounder records from Greenland, Fig. 8). Regardless of the explanation, we are encouraged that it is possible to use the GLAS data to identify likely "false positive" or "low accumulation" events and to measure an insignificant accumulation by the same methodology we employ to measure the amount of new snow in "normal" events.

7. Future work

We do not claim to have solved this problem completely. There is a clear need for refinements to the technique. There is still a strong influence of surface temperature on the temporal variation of the 85V data. Additionally, melting of surface snow is known to initially increase brightness temperature, but in Antarctica this effect is limited to the edges of the continent (Zwally & Fiegles, 1994). Independent measurements of surface temperature would be valuable on both counts, allowing the calculation of an effective emissivity and determining when melt occurs. Direct measurements of surface temperature are available when clouds are absent, but new snow falls from clouds, increasing the need for techniques to determine surface temperature beneath clouds.

Our methodology also does not remove cases of altered surface emission caused by factors other than new snow accumulation, our "false positives". The most common process likely is horizontal advection or ablation of surface snow. Because no new snow is generated, this process would presumably involve ablation in one area and accumulation in another area. In the absence of ground validation data, we cannot be certain of the nature of the altered brightness temperatures. If both areas are contained within the area analyzed by laser altimeter crossovers, a zero-accumulation result would be expected, but might miss the regional gradient between the mass-gain area and the mass-loss area. Coincident wind data might add value to the analysis, leading to an ability to resolve horizontal wind transport of snow.

The ICESat/GLAS data set is still being refined to account for factors limiting its precision and/or accuracy. More critically, limited periods of ICESat/GLAS operation restrict our ability to complete an extensive temporal study of accumulation on ice sheets. Improved laser altimetry, especially continuous operation leading to more crossover data, will lead to improved quantification of new-snow amounts in space and time. Similarly useful data could also be provided by the upcoming Cryosat radar altimeter.

8. Summary

We have demonstrated a new methodology to utilize a combination of remote sensing data to measure the temporal and spatial pattern of new snowfall on ice sheets as well as the thickness of new snow. The vertically polarized brightness temperature at 85 GHz is extremely sensitive to changes caused by the introduction of new, more emissive snow over an aged surface of metamorphosed, more rounded and, therefore, less emissive snow. Over the cold and high-elevation ice sheets the atmospheric contribution due to water vapor, including clouds, is relatively constant at 10 to 13 K and its daily variation is 1 K or less. Temperature changes are more important and directly affect 85 GHz brightness temperatures. Their day-to-day variation is usually only a few Kelvin, less than the observed larger variation in brightness temperature associated with new snow. The Hilbert–Huang Transform (HHT) diminishes many of the undesirable temporal variations of the 85V data and improves the detection of new snow events. Our technique identifies nearly every new snow event observed by field personnel at Siple Dome station in West Antarctica and matches well with acoustic sounder data in Dronning Maud Land. In meteorologically complex regions, such as at McMurdo Station, the ability to detect new snow events is diminished but still significant. Having detected when and where new snow likely occurs, elevation differences at groundtrack crossovers from satellite laser altimeter observations then are used to supply a useful statistical measure of new snow amount.

We believe this work sets out a new direction towards an eventual capability to systematically and comprehensively measure new snow on ice sheets. It is independent of season and, we hope, will eventually lead to routine measurements of new snow and the construction of the climatology of new snow accumulation on ice sheets.

Acknowledgments

The University of Wisconsin AMRC provided the meteorological records used in this work. We thank the following individuals for various data used in this work: David Bromwich and Jason Box for providing the ERA-40 product for the region around Siple Dome; Carleen Reijmer and Michiel van den Broeke for AWS and acoustic sounder data from Dronning Maud Land and Jay Zwally for supplying the file of ICESat crossover differences. Radiosonde data were made available by the British Antarctic Survey and downloaded via the web. This work was supported by a grant from NASA's Cryospheric Program.

References

Abdalati, W., & Steffen, K. (1997). Snowmelt on the Greenland ice sheet as derived from passive microwave satellite data. *Journal of Climate*, *10*(2), 165–175.

Arcone, S. A., Spikes, V. B., Hamilton, G. S., & Mayewski, P. A. (in press). Stratigraphic continuity in 400-Mhz radar profiles in West Antarctica. *Ann. Glaciol*., 39.

Bales, R. C., McConnell, J. R., Mosley-Thompson, E., & Csatho, B. (2001). Accumulation over the Greenland ice sheet from historical and recent records. *Journal of Geophysical Research*, *106*(D24), 33,813–33,825.

Black, H. P., & Budd, W. (1964). Accumulation in the region of Wilkes, Wilkes Land, Antarctica. *Journal of Glaciology*, *5*(37), 3–15.

Bromwich, D. H., Chen, Q., Bai, L., Cassano, E. N., & Li, Y. (2001). Modeled precipitation variability over the Greenland ice sheet. *Journal of Geophysical Research*, *106*(D24), 33,891–33,908.

Cavalieri, D. J., Gloersen, P., & Campbell, W. J. (1984). Determination of Sea Ice Parameters with the NIMBUS-7 SMMR. *Journal of Geophysical Research-Atmospheres*, *89*(ND4), 5355–5369.

Giovinetto, M. B., & Zwally, H. J. (2000). Spatial distribution of net surface accumulation on the Antarctic ice sheet. *Annals of Glaciology*, *31*, 171–178.

Goita, K., Walker, A., & Goodison, B. (2003). Algorithm development for the estimation of snow water equivalent in the boreal forest using passive microwave data. *International Journal of Remote Sensing*, *24*(5), 1097–1102.

Gow, A. J., & Rowland, R. (1965). On the relationship of snow accumulation to surface topography at "Byrd Station", Antarctica. *Journal of Glaciology*, *5*(42), 843–847.

Huang, N. (1998). The empirical mode decomposition and the Hilbert spectrum for nonlinear and non-stationary time series analysis. *Proceedings of the Royal Society of London. A*, *454*, 903–995.

Kaleschke, L., Lupkes, C., Vihma, T., Haarpaintner, J., Bochert, A., Hartmann, J., et al. (2001). SSM/I sea ice remote sensing for mesoscale ocean–atmosphere interaction analysis. *Canadian Journal of Remote Sensing*, *27*, 526–537.

Kummerow, C. (1993). On the Accuracy of the Eddington Approximation for Radiative transfer in the Microwave Frequencies. *Journal of Geophysical Research*, *98*(D2), 2757–2765.

Markus, T., & Burns, B. A. (1995). A method to estimate sub-pixel scale coastal polynyas with satellite passive microwave data. *Journal of Geophysical Research*, *100*, 4473–4487.

Markus, T., & Cavalieri, D. J. (2000). An enhancement of the NASA Team sea ice algorithm. *IEEE Transactions on Geoscience and Remote Sensing*, *38*, 1387–1398.

Nakaya, U. (1954). *Snow crystals: Natural and artificial*. Cambridge: Harvard University Press.

Reijmer, C. H., & van den Broeke, M. R. (2003). Temporal and spatial variability of the surface mass balance in Dronning Maud Land, Antarctica, as derived from automatic weather stations. *Journal of Glaciology*, *49*(167), 512–520.

Richardson, C., & Holmlund, P. (1999). Spatial variability at shallow snow-layer depths in central Dronning Maud Land, East Antarctica. *Annals of Glaciology*, *29*, 10–16.

Rott, H., Sturm, K., & Miller, H. (1993). Active and passive microwave signatures of Antarctic firn by means of field measurements and satellite data. *Annals of Glaciology*, *17*, 337–343.

Shuman, C. A., & Alley, R. B. (1993). Spatial and temporal characterization of hoar formation in central Greenland using SSM/I brightness temperatures. *Geophysical Research Letters*, *20*(23), 2643–2646.

Shuman, C. A., Alley, R. B., & Anandakrishnan, S. (1993). Characterization of a hoar-development episode using SSM/I brightness temperatures in the vicinity of the GISP2 site, Greenland. *Annals of Glaciology*, *17*, 183–188.

Shuman, C. A., Alley, R. B., Fahnestock, M. A., Fawcett, P. J., Bindschadler, R. A., Anandakrishnan, S., et al. (1997). Detection and monitoring of annual indicators and temperature trends at GISP2 using passive microwave remote sensing data. *Journal of Geophysical Research*, *102*(C12), 26877–26886.

Shuman, C. A., Zwally, H. J., Schutz, B. E., Brenner, A. C., DiMarzio, J. P., & Suchdeo, V. P., (submitted for publication). Ice sheet elevations from ICESat 2003–2005, *Geophysical Research Letters*, (ICESat Special Issue Volume 1).

Skofronick-Jackson, G. M., Kim, M. J., Weinman, J. A., & Chang, D. E. (2004). A physical model to determine snowfall over land by microwave radiometry. *IEEE Transactions on Geoscience and Remote Sensing*, *42*(5), 1047–1058.

Svendsen, E., Matzler, C., & Grenfell, T. C. (1987). A model for retrieving total sea ice concentration from a spaceborne dual-polarized passive microwave instrument operating at 90 GHz. *International Journal of Remote Sensing*, *8*, 1479–1487.

Vaughan, D. G., Bamber, J. L., Giovinetto, M. B., Russell, J., & Cooper, A. P. R. (1999). Reassessment of net surface mass balance in Antarctica. *Journal of Climate*, *12*(4), 933–946.

Whillans, I. M. (1975). Effect of inversion winds on topographic detail and mass balance on inland ice sheets. *Journal of Glaciology*, *14*(70), 85–90.

Zwally, H. J., & Brenner, A. C. (2001). In L. L. Fu, & A. Cazenave (Eds.), *Ice sheet dynamics and mass balance, satellite altimetry and earth sciences* (pp. 351–369). Academic Press.

Zwally, H. J., & Fiegles, S. (1994). Extent and duration of Antarctic surface melt. *Journal of Glaciology*, *40*(136), 463–476.

Zwally, H. J., Schutz, B., Abdalati, W., Abshire, J., Bentley, C., Brenner, A., et al. (2002). ICESat's laser measurements of polar ice, atmosphere, ocean and land. *Journal of Geodynamics*, *34*, 405–445.